8-2018

# Comparing Laser Assisted Pulling and Chemical Vapor Deposition Methods in the Fabrication of Carbon Ultramicro- and Nanoelectrodes

Theophilus Neequaye
*East Tennessee State University*

# Comparing Laser-Assisted Pulling and Chemical Vapor Deposition Methods in the Fabrication of Carbon Ultramicro- and Nanoelectrodes

---

A thesis

presented to

the faculty of the Department of Chemistry

East Tennessee State University

In partial fulfillment

of the requirements for the degree

Master of Science in Chemistry

---

by

Theophilus Neequaye

August 2018

---

Dr. Gregory W. Bishop, Chair

Dr. Dane W. Scott

Dr. Marina Roginskaya

Keywords: ultramicroelectrodes, electrochemistry, nanopipette, chemical vapor deposition, carbon fiber

ABSTRACT

Comparing Laser Assisted Pulling and Chemical Vapor Deposition Methods in the Fabrication of Carbon Ultramicro- and Nanoelectrodes

by

Theophilus Neequaye

Ultramicroelectrodes (UMEs) (limiting dimensions <~25 µm) and nanoelectrodes (<~100 nm) exhibit enhanced electrochemical properties compared to macroscopic electrodes. Their small sizes and enhanced properties make them well-suited for various interesting and important applications such as measuring redox-active species in nonaqueous solvents, studying intermediates of fast electrochemical reactions, and investigating electrochemical and electrocatalytic properties of single nanoparticles. While UMEs are commercially available, nanoelectrode fabrication is still largely confined to research labs. Various methods for constructing nanoelectrodes have been reported and continue to be developed, but most require considerable expertise, and comparisons between different fabrication processes are lacking. In this work, a comparison of laser-assisted pulling and chemical vapor deposition (CVD) methods of electrode fabrication is made with the aim of optimizing production of carbon nanoelectrodes for single nanoparticle electrochemical measurements. By examining effects of pulling parameters, post-pulling treatments, and CVD processing, electrodes as small as ~50 nm were successfully produced.

DEDICATION

This work is dedicated to Mr. Kenneth Owusu, Cecilia Sam, Albert Wilson Smith, and my family for their advice, support and encouragement through the challenges of life.

ACKNOWLEDGMENTS

If it had not been the Lord on my side, let Israel say (Psalm 124:1). My greatest thanks and appreciation goes to the almighty God for the love, protection and numerous blessings He has bestowed on me. Father, my mouth will continually sing your praises. My endless and sincere gratitude goes to my supportive research advisor, Dr. Gregory Bishop who consistently and painstakingly guided and encouraged me throughout this research work. I will be forever indebted to Dr. Marina Roginskaya and Dr. Dane Scott for availing themselves to serve as advisory committee members on my thesis and also shaping me up as a young chemist. I thank Rev. Dr. Arnold Nyarambi for his guidance and encouragement. I also thank the American Chemical Society Petroleum Research Fund (Award # 58123 – UNI5) and the Office of Research and Sponsored Programs at East Tennessee State University for financial support of this project. Finally, my appreciation goes to all students in Dr. Bishop's research group especially my research partner George Affadu-Danful.

TABLE OF CONTENTS

LIST OF TABLES

Table Page

LIST OF FIGURES

Figure Page

# LIST OF ABBREVIATIONS

AuNPs – Gold nanoparticles

CV – Cyclic voltammetry

CVD – Chemical vapor deposition

FcMeOH – Ferrocenemethanol

ID – Inner diameter

OD – Outer diameter

SEM – Scanning electron microscopy

TEM – Transmission electron microscopy

UMEs – Ultramicroelectrodes

# CHAPTER 1

# INTRODUCTION

## Nanoparticles and Catalysis

Many important chemical processes such as those involved in the production of fuels, control of emissions from industrial vehicle operation, and production of effective pharmaceuticals have been improved over the years due to advances and continuing development of catalysts that promote crucial reactions.[1] Nanoparticles have been widely employed and intensely studied for their catalytic properties, which can be attributed to their large surface area-to-volume ratios.

Research aimed at determining the relationships between physical and catalytic properties of nanoparticles is most often carried out using collections of nanoparticles deposited on a solid support.[2] However, ensemble measurements that are generated by these types of studies may create an important barrier in nanoparticle characterization and optimization.[3] Complex considerations such as interparticle distance, nanoparticle loading, and heterogeneity in nanoparticle size and structure are often unavoidable for systems of multiple nanoparticles. These parameters are typically difficult to control and characterize, making it challenging or impossible to accurately determine connections between nanoparticle properties and catalytic activity, since measurements obtained from multi-particle systems represent an ensemble average of nanoparticle properties combined with aspects of particle distribution. In contrast, studies of the catalytic properties of nanoparticles at the single nanoparticle level should produce results that are easier to interpret and allow a more direct approach to evaluating the nanoparticle structure-function relationship.[4]

## Measuring Electrocatalytic Properties of Single Nanoparticles

There are considerable challenges associated with single nanoparticle measurements due to the difficulty in isolating single small particles and distinguishing low levels of signal produced at a

nanoparticle from background. However, recent advances in electrochemical techniques have enabled evaluation of the electrocatalytic properties of individual nanoparticles.[5] These electrocatalytic measurements carried out at single nanoparticles have been performed through evaluation of transient currents that develop as single nanoparticles impact ultramicroelectrodes (electrodes with limiting dimensions $\leq 25$ μm)[6] and through single nanoparticle voltammetry accomplished by immobilizing single nanoparticles on nanometer-sized electrodes.[2]

Nanoparticle Impact Studies

The Bard research group[6] and others[7-15] have demonstrated electrochemical measurements of single metal nanoparticles through evaluation of current time (*i*-*t*) transients that are produced when nanoparticles collide with an ultramicroelectrode (Figure 1). In these experiments, termed nanoparticle impact studies, the ultramicroelectrode is held at a potential that is insufficient to drive an electrochemical reaction. However, signal in the form of current is produced by a single nanoparticle as it comes into contact with the electrode surface, where the nanoparticle can undergo direct redox reaction or is able to catalyze the electrochemical conversion of reactant to product at the applied potential.

Nanoparticle impact methods require the measurement of small current transients that develop as nanoparticles collide with the electrode surface due to random Brownian motion.[16,17,18] The *i*-*t* response consists of a series of discrete steps for nanoparticles that irreversibly adhere to the electrode surface after collision and catalyze the electrochemical reaction once adsorbed, or a collection of short pulses (also called spikes or blips[16]) for individual nanoparticles that either only come into contact with the electrode for a short period of time or get poisoned once they adsorb onto the electrode surface.[17] The magnitude of a current step or spike is proportional to a particle's size.[19]

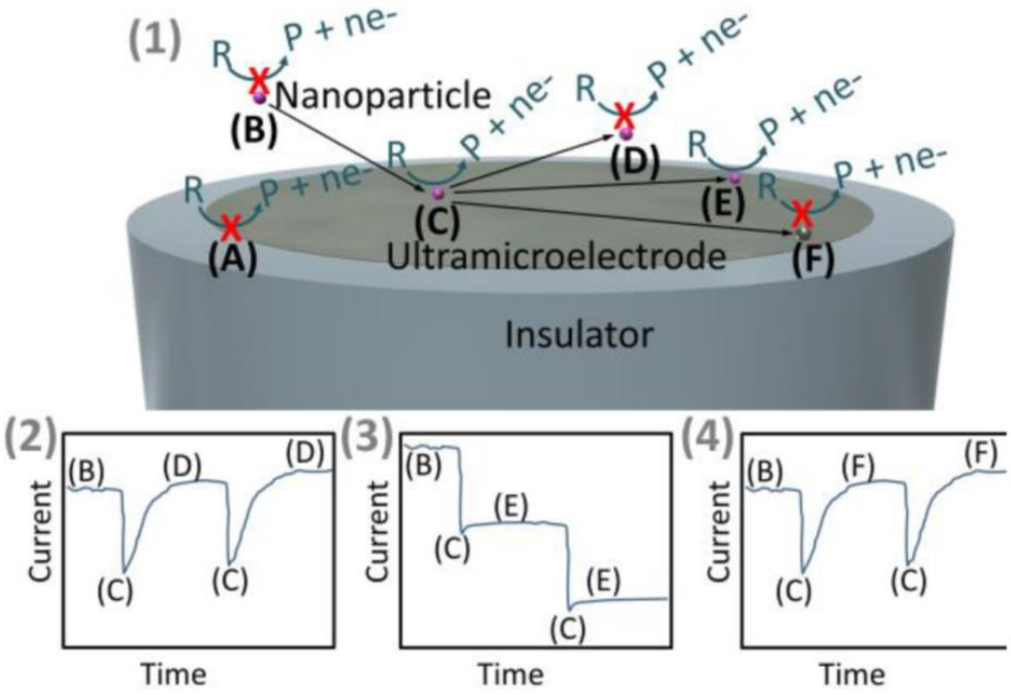


**Figure 1:** Illustrated schematic of nanoparticle impact method and typical responses. (1) The ultramicroelectrode is held at a potential that is unable to directly oxidize reactant R to product P (A). The n-electron oxidation reaction is also prohibited at nanoparticles far away from the electrode surface (B). Upon collision with the electrode surface, the nanoparticle is able to catalyze the reaction (C) and an oxidation current is observed (2-4). The particle may then either leave the surface (D) resulting in a spike-type response (2); remain on the surface (E) resulting in a staircase response (3); or become poisoned on the surface (F) resulting in a spike-type response (4).

Single Nanoparticle Voltammetry

Electrochemical behavior of single nanoparticles can also be determined by employing nanoelectrodes. Restricting electrode size such that it is comparable to the size of the particle of interest ensures that only a single nanoparticle can be attached to the surface.[3] Nanoparticles may be deposited through covalent bonding, adsorption onto electrode surfaces modified with appropriate chemical linkers, or by direct reduction of metal ions on bare electrode surfaces.[20,21]

Zhang et al. studied electrocatalysis of the oxygen reduction reaction by single AuNPs attached to silane-modified Pt nanoelectrodes.[22] Enhancement in current associated with oxygen reduction at AuNPs confirmed the electrocatalytic behavior of AuNPs. Electrocatalytic activity was

also supported by the positions of half-wave potentials which were 135-335 mV more positive than that for same reaction at bare Pt nanoelectrodes. In a separate study, Mirkin et al. reported on the electrocatalytic behavior of single AuNPs on carbon nanoelectrodes for the hydrogen evolution reaction and compared results to that of ensemble gold particles.[2] The onset of current for the hydrogen evolution reaction at ensemble AuNPs occurs at a potential that is significantly more negative compared to that of the single 10 nm gold particle, confirming the electrocatalytic behavior of a single AuNP.

## Electrodes for Single Nanoparticles Measurements

Both nanoparticle impact and voltammetric measurements of immobilized single nanoparticles require small electrodes (UMEs and nanoelectrodes, respectively) as platforms for electrochemical measurements. UMEs that are employed for nanoparticle impact studies have been around since the 1980s and are now commercially available. Wightman[23,24] and others[25,26] discovered certain advantageous properties such as very small IR drop and small $RC_{dl}$ time constants ($C_{dl}$ is double layer capacitance) for UMEs, which have led to their widespread use for applications such as measuring redox-active species in low-conductivity solvents, studying intermediates in fast electrochemical reactions, and investigating electrochemical and electrocatalytic properties of single nanoparticles through nanoparticle impact measurements.

Reports on fabrication of nanometer-sized electrodes first appeared in the mid-1980s,[27] and many types of nanometer-sized electrodes with different geometries such as inlaid disk, ring, hemisphere, sphere, and conical produced by various fabrication techniques have since been described. However, production of these small electrodes is still largely confined to research labs.[28-30] Generally, nanoelectrode fabrication can be grouped under two main methods. These are bottom-up and top-down approaches. Top-down fabrication methods involve insulating or removing

material from bulk objects to produce smaller entities while bottom-up approaches correspond to attaching small building blocks together to yield a small object.

Top-Down Fabrication of Nanoelectrodes

Insulation of metal wire or carbon fiber followed by careful, controlled exposure through chemical etching or mechanical polishing is representative of top-down fabrication methods.[31-34] A well-explored top-down method is the laser-assisted pulling technique from which platinum, gold, silver, and carbon fiber electrodes have been made.[35-37] In the laser-assisted pulling method, a thin wire or carbon fiber (~7-100 μm in diameter) is inserted into a capillary tube. A laser pulse is used to heat the glass tube, creating a seal. Then, a second laser pulse is applied while pulling the tube from each end to separate the tube and wire or fiber into two parts with tapered ends in which the conductive wires or fibers are completely or partially sealed.[38] Careful removal of the insulating glass layer to expose the conductive element produces ultramicro- or nanoelectrodes.

Reported carbon fiber and metal wire exposure techniques include flame etching, chemical etching, and mechanical polishing. Wightman[39] pioneered the use of flame as a post-pulling treatment technique to fabricate electrodes with diameters of about 2 μm. Further advancement made by Huang et. al[40] produced carbon fiber electrodes with tip size of about 100 nm. Zhang et al. used argon ion beam as an etching method to fabricate carbon fiber nanoelectrodes with tip radii dimensions ranging from 25 to 250 nm.[41] Li et al. electrochemically etched carbon fiber in NaOH solution before inserting it into a glass capillary to produce ultra-small disk-shaped electrodes.[42] Agyekum et al.[43] chemically etched glass to expose platinum wire using hydrofluoric acid in their preparation of a 6 nm platinum nanoelectrode.

Bottom-Up Fabrication of Nanoelectrodes

An example bottom-up fabrication technique is the pyrolysis of gases such as methane and butane inside a capillary tube with a very small internal diameter such as a nanopipette produced from laser-assisted pulling of a glass capillary tube.[44] In this method, carbon is deposited inside the small capillary tube through chemical vapor deposition.[45-48] Mirkin et al. reported carbon nanoelectrodes with diameters as small as ~4 nm by pyrolysis of methane in quartz nanopipettes at 875 ºC for 30 min in a tube furnace.[49] Actis et al. used an inexpensive butane microtorch to deposit carbon inside quartz nanopipettes from a propane/butane mixture.[44] Baker et al. produced carbon nanoelectrodes with planar and three-dimensional geometries by CVD of parylene C in nanopipettes with internal diameters as small as 150 nm at the tapered end.[50]

Aggregation of nanoparticles in a restricted space such as within a nanopipette is another bottom-up method used to fabricate metal nanoelectrodes. Under controllable experimental conditions, this line of bottom-up method gives added advantage in production cost for metal nanoelectrodes compared to top-down approaches since minimal quantities of nanoparticles are required and metal nanoparticles are often less expensive than precious metal wires. Demaille et al. reported the use of dithiol as a linking agent to fill up the orifice of a pipette with AuNPs in the fabrication of gold microelectrodes.[51] Also, Jena et al.[52] and the Mirkin group[53] fabricated nanoelectrodes by sealing metal nanoparticles in nanopores.

Comparison of Nanoelectrode Fabrication Strategies

Overall, several nanoelectrode fabrication strategies have been reported (Table 1). Vast improvements have been made over the years in terms of electrode size and robustness. However, fabrication challenges like production cost, reproducibility, and production of more controllable geometries persist.[38]

**Table 1**: Selected fabrication strategies for preparing disk-shaped nanoelectrodes.

| Authors | Material | Fabrication Strategy | Radius (nm) |
|---|---|---|---|
| Hao et al.[54] | Gold | Electroplating in nanopipette | 20 |
| Chen et al.[55] | Carbon | CVD of $CH_4$/focused-ion beam milling | 50 |
| Schroeder et al.[39] | Platinum | Laser-assisted pulling Pt wire/HF etching | 6 |
| Macpherson et al. [29] | Silver | Deposition nanoparticles in nanopipette | 10 |
| Li et al.[56] | Platinum | Laser-assisted pulling Pt wire | 1 |
| Anderson et al.[57] | Carbon | CVD/HF etching | 25 |
| Fei et al.[58] | Carbon | Electrochemical etching/ C fiber | 50 |
| Sun et al.[33] | Carbon | Laser-assisted pulling C fiber | 25 |
| Oja et al. [20] | Platinum | Laser-assisted pulling Pt wire | 100 |
| Takahashi et al.[46] | Carbon | CVD of $CH_4$ using furnace | 2 |
| Morton et al. [50] | Carbon | CVD of parylene C | NR[a] |
| Actis et al.[44] | Carbon | CVD of mixed $C_3H_8$/$C_4H_{10}$ using microtorch | 10 |

[a]Not Reported

## Research Objectives

Electrochemical measurements of single nanoparticles can provide information about the relationship between nanoparticle structure and function, which is necessary to design and optimize nanoparticle electrocatalysts. Carbon is desirable as a material for producing nanoelectrodes to study electrochemical behavior of single metal nanoparticles through immobilization strategies since carbon is relatively inert towards many important electrochemical reactions catalyzed by metal nanoparticles.[2] In this work, carbon ultramicroelectrodes were fabricated through two different pathways, laser-assisted pulling of carbon fiber and chemical vapor deposition of carbon in nanopipettes, in an effort to optimize conditions for producing electrodes capable of studying electrocatalytic behaviors of single nanoparticles. Effects of pulling parameters, post-pulling treatment strategies such as flame etching and manual polishing, and CVD processing on electrode size were investigated. Electrodes as small as ~50 nm were successfully produced. Future efforts will be directed towards further reducing electrode size, improving the reproducibility of electrode fabrication, and exploring nanoparticle immobilization strategies.

# CHAPTER 2

# EXPERIMENTAL

## Materials

All chemicals were used as received from the manufacturer. Ferrocenemethanol (FcMeOH, ≥97%) was obtained from Acros Organics and potassium chloride (99+%) from Sigma-Aldrich. Borosilicate glass (O.D 1.0 mm, I.D 0.58 mm) and quartz glass (O.D 1.0 mm, I.D 0.30 mm) capillaries were purchased from Sutter Instrument Co. (Novato, CA). Silver conductive adhesive paste was obtained from Beantown Chemical (Hudson, NH) and nichrome wire from Parr Instrument Co. (Moline, IL). Carbon fiber (7 µm in diameter) was purchased from Goodfellow Cambridge Limited (Huntington, England). Butane/propane mix (30:70) used for CVD was purchased from Coleman Co. Inc. (Wichita, KS). All aqueous solutions were prepared using 18.2 MΩ·cm ultrapure water, which was obtained by passing deionized water through a Millipore Synergy purification system.

## Preparation of Carbon Fiber Electrodes

Carbon fiber ultramicroelectrodes (CFUMEs) were fabricated using borosilicate glass capillaries and a laser-assisted pipette puller (Sutter Instruments P- 2000). First, a collection of carbon fibers (~10 cm in length) (Figure 2A) was washed with ethanol, acetone and distilled water.[40] The fibers were subsequently dried in an oven at 60˚C for 30 min. A single carbon fiber was then carefully separated from the pre-treated bunch and inserted in a borosilicate glass capillary through vacuum aspiration. Successful incorporation of the fiber in the capillary was verified by viewing the capillary under a Nikon microscope interfaced with a Pixlink CCD camera that was connected to a computer (Figure 2B).

The ultimate size and tip shape of an electrode prepared using the laser-assisted pulling method greatly depends on the applied pulling parameters. Though several research works have reported pulling parameters that produced small functional electrodes for various applications using P-2000 pullers,[43,44,55] values associated with pulling settings are unitless and each puller is unique.[59] Therefore, pulling parameters, which include HEAT, FILAMENT, VELOCITY, DELAY, and PULL, must be adjusted in order to obtain desired electrode size and shape.

The HEAT value which ranges from 0 to 999 represents the output power of the laser and the amount of energy directed onto the capillary glass. FILAMENT value determines the scanning pattern of the laser beam with lower values representing smaller scanning areas and higher values corresponding to larger scanning areas. VELOCITY is noted for the speed at which the puller bar moves before executing the hard pull. DELAY and PULL parameters control the timing of the start of the hard pull relative to the deactivation of the laser and the force of the hard pull, respectively.[60]

With the aid of the pipette puller and suitable pulling parameters, the capillary was separated into two parts. Vacuum was applied to each of the two open ends of the capillary throughout the heating and pulling process so that the carbon fiber could be sealed in the glass capillary (Figure 2C), producing two carbon fiber electrodes. Conductive silver paste was applied to a nichrome wire, which was then inserted into the open end of each pulled electrode to make contact with the carbon fiber inside the capillary tube and create an external connection for connecting the electrode to the electrochemical workstation (Figure 2D). Epoxy was used to seal the open end of the capillary and hold the external wire in place. Epoxy was left to dry overnight prior to electrode use.

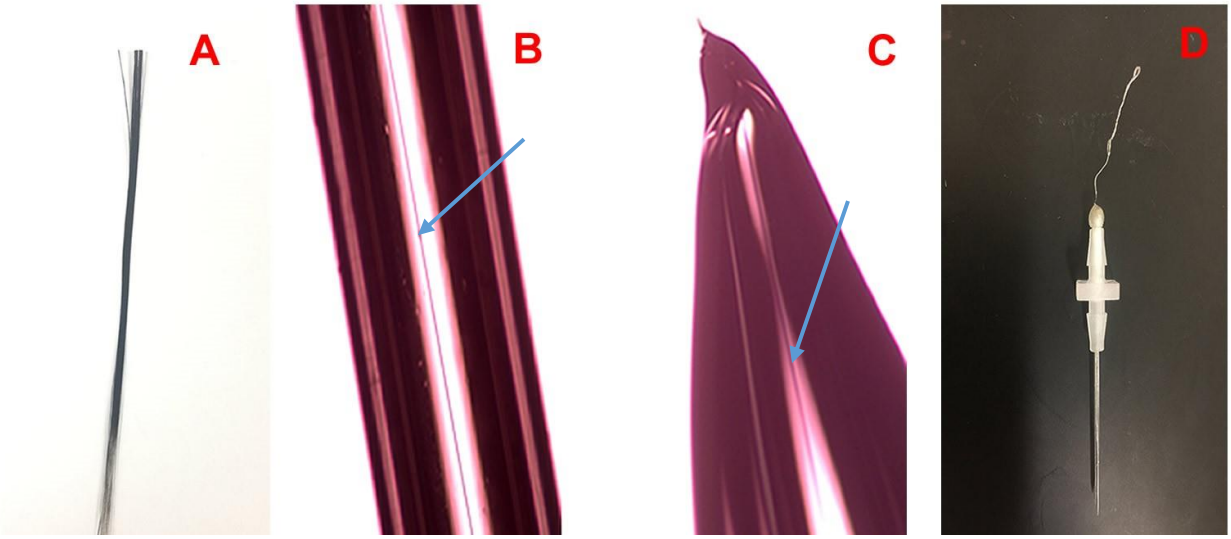


**Figure 2:** Stages of carbon fiber ultramicroelectrode fabrication by laser-assisted pipette pulling. A) Bunch of carbon fibers washed with acetone, ethanol and distilled water. B) Single carbon fiber inserted in a borosilicate glass capillary. C) Sealed carbon fiber in a pulled borosilicate glass capillary. D) Fabricated electrode with nichrome connection wire. Blue arrows in B and C indicate location of the carbon fiber.

Preparation of Carbon UMEs Using CVD Method

Pipettes with tapered tip openings were pulled from a quartz capillaries using the laser-assisted pipette puller. Carbon was deposited into the nanopipette through a previously described chemical vapor deposition (CVD) fabrication process (Figure 3).[61] The larger untapered end of the nanopipette was connected to a propane/butane mixture using Tygon tubing, and the smaller opening was placed in the path of a low opposing flow of argon. A butane flame from a microtorch (Bernzomatic) was directed onto the smaller opening of the nanopipette to carry out pyrolysis of the flowing propane/butane mixture inside the capillary for about 20 s to deposit a layer of carbon in the pipette (Figure 4). Electrical connection to the deposited carbon was achieved by inserting a stainless steel or nichrome wire into the unfilled end of the capillary tube so that it contacted the deposited carbon at the tapered end.

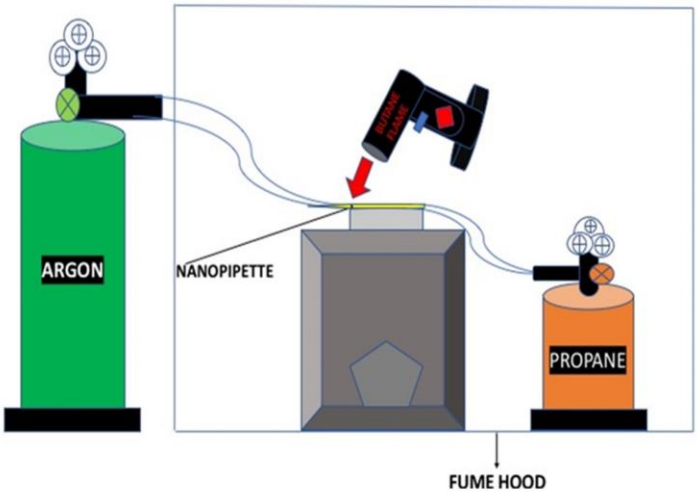


**Figure 3:** Schematic representation of CVD of carbon in a nanopipette to produce ultramicroelectrodes

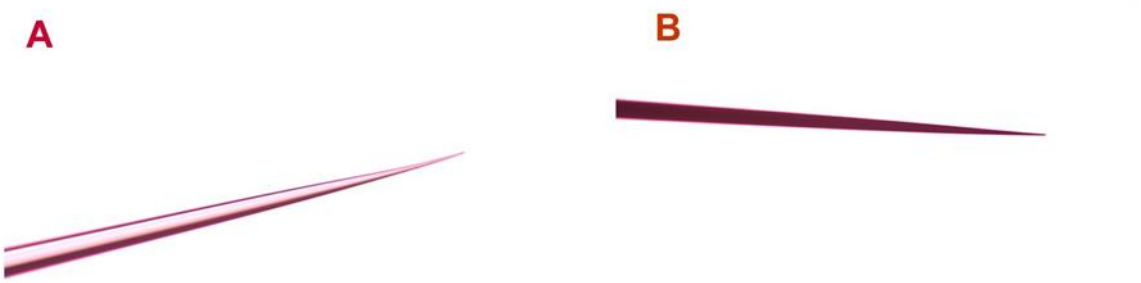


**Figure 4:** Images of pulled quartz nanopipette and CVD carbon electrode. Pulled pipette before (A) and after (B) carbon deposition.

Post-Pulling Treatment Techniques for Electrodes

Manual mechanical polishing and butane flame etching were the two post-pulling treatment strategies employed to expose carbon fibers which were sealed in borosilicate glass by the pulling process. Fabricated electrodes were carefully polished on an 800-grit abrasive paper by hand to produce disk-shaped electrodes. Electrochemical responses of electrodes were tested after every 2 min of polishing to monitor the polishing process. Breaking of electrode tip because of vigorous polishing and improper handling is a major challenge encountered in employing this post-pulling

treatment method as well as other frequently used mechanical fiber exposure methods such as beveling by use of a motor-controlled, rotating polishing disk.

Flame etching was carried out by using a butane microtorch. The flame was applied to the small tip opening of the pulled borosilicate capillary containing the sealed carbon fiber for a time of approximately 5 s to melt the glass and etch the carbon fiber. This procedure was repeated for a number of times until the desired electrochemical response that indicated a functioning electrode was obtained.

## Characterization of Electrodes

It is very important to completely characterize the shape and size of nanoelectrodes because small variations in their geometries can cause differences in their electrochemical response. Electron microscopy techniques such as transmission electron microscopy (TEM) and scanning electron microscopy (SEM) as well as electrochemical methods are mainly used in characterizing nanoelectrodes.[22] It is mostly challenging to completely characterize nanoelectrodes with adequate spatial resolution using electron microscopy because of the small sizes of the conductive electrode surface and extensive charging effects from the surrounding glass insulator.

In these studies, sizes of fabricated electrodes were determined via the electrochemical method of cyclic voltammetry (CV). A two-electrode system was used for CV measurements with Ag/AgCl (in 3 M NaCl) serving as the reference/counter electrode and the carbon electrode as the working electrode. All measurements were carried out at room temperature using a Bioanalytical Systems Inc. Epsilon electrochemical workstation.

Unlike typical macroelectrodes, which exhibit peak-shaped CV responses for redox reactions due to linear diffusion,[62] ultramicro- and nanoelectrodes produce sigmoidal-shaped CVs for faradaic reactions due to the dominance of radial diffusion in mass transport to and from the

electrode surface.[62] The steady-state limiting currents obtained from CVs of disk-shaped ultramicro- and nanoelectrodes in aqueous solutions of common redox probes can be used to estimate the electrode radius via the equation:

$$i_{ss} = 4nFDcr \quad (1)$$

Where $i_{ss}$ is the steady-state limiting current, $n$ is number of electrons involved in the redox reaction, $F$ is Faraday's constant (96,484.56 C/mol at 25 $^{o}$C), $r$ is electrode radius in cm, $D$ is diffusion coefficient of the redox probe in $cm^2/s$, and $c$ is the bulk concentration of the redox probe in $mol/cm^3$. In these studies, sizes of carbon electrodes were determined via equation 1 using the one-electron oxidation of the common redox probe ferrocene methanol, which has a diffusion coefficient of $7.6 \times 10^{-6}$ $cm^2/s$.[49]

# CHAPTER 3

# RESULTS AND DISCUSSION

## Pulling Parameters and Electrochemical Responses

Fabrication of nanometer-sized electrodes through laser-assisted pulling techniques depends greatly on the applied pulling parameters and the type of glass capillary used.[63] Though many different sets of pulling parameters were tested, four different combinations (programs A-D in Table 2) were found to adequately seal carbon fibers in borosilicate glass capillaries. Another combination of settings (program E in Table 2) also seemed to mostly produce sealed carbon fibers, but exhibited long fragile tapered tips (Figure 5).

**Table 2:** Pulling parameters used in making carbon fiber ultramicroelectrodes

| Program | Heat | Filament | Velocity | Delay | Pull |
|---|---|---|---|---|---|
| A | 450 | 0 | 18 | 20 | 0 |
| B | 330 | 3 | 30 | 220 | 0 |
| C | 450 | 1 | 15 | 80 | 0 |
| D | 500 | 1 | 20 | 150 | 0 |
| E | 450 | 1 | 15 | 80 | 50 |

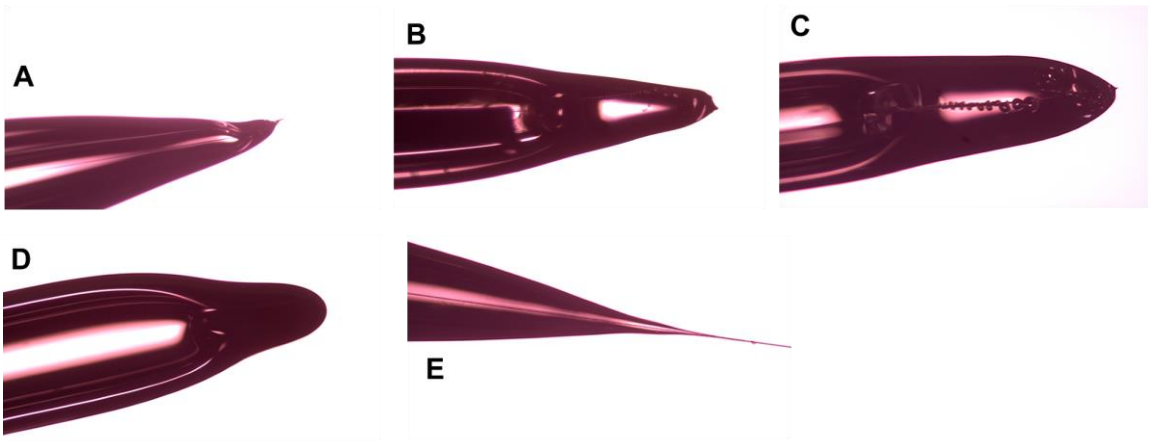


**Figure 5:** Representative images of carbon fibers sealed in borosilicate capillaries prepared by laser-assisted pulling. Images A-E correspond to sealed fibers obtained from pulling parameters A-E listed in Table 2.

One of the most important pulling parameters for obtaining robust and well-sealed fibers was the pull value, which largely controls the taper of the pulled capillary. Programs with pull values > 0 typically produced fragile, tapered electrode tips (Figure 5E) that were not functional as the tapered tip typically broke as a result of electrode handling. Programs that included pull value = 0 generally enabled effective sealing of the fiber in the borosilicate glass and produced electrodes with blunt, resilient ends. Since the puller bars tend to naturally pull apart and draw out the glass upon heating of the capillary even with pull values of 0, a piece of copper wire wrapped around the capillary clamp adjustment screws on the puller arms or a puller bar stopper[54] was used to limit the motion of the puller bars during the sealing process for programs with pull values of 0.

Of the four different pulling programs found to effectively seal carbon fibers in glass capillaries and also produce durable, and stable electrodes, only one program (program A) produced electrodes that exhibited electrochemical response towards FcMeOH/$FcMeOH^+$ redox couple without any post-pulling treatment (Figure 6). In contrast, electrodes prepared using pulling programs B, C, and D exhibited no faradaic current when electrochemical response towards FcMeOH was tested immediately after fabrication, indicating that the carbon fiber was completely sealed in glass and not accessible to the diffusible redox species in solution.

Interestingly, the small currents measured for the oxidation of FcMeOH at the electrode prepared using program A suggest that an UME was produced. However, the CV contained a pair of peaks associated with the FcMeOH/$FcMeOH^+$ redox couple, which indicates a relatively slow transport process and is not consistent with UME behavior since UMEs are known to exhibit sigmoidal CV response due to fast radial diffusion that dominates transport. This unexpected peak-shaped response with low current was also observed by Velmurugan et al.[64] for platinum nanoelectrodes prepared by laser-assisted pulling. This behavior is indicative of the presence of a

thin layer of glass covering the electrode, which increases viscosity near the electrode surface due to the presence of a hydrated glass gel layer and inhibits transport of the redox species.[64]

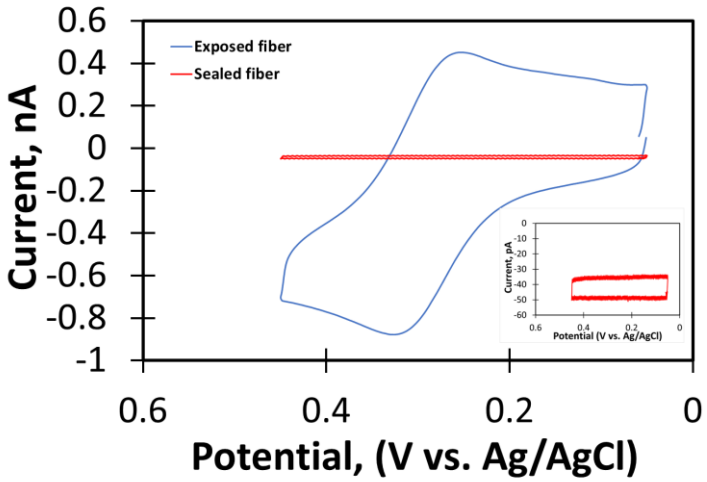


**Figure 6:** Cyclic voltammograms for sealed carbon fiber electrodes in 0.5 mM FcMeOH with 0.1 M KCl. Responses obtained from electrode with exposed fiber made from pulling program A (blue line) and from electrode with completely sealed fiber made from pulling program C (red line). Electrodes made from pulling programs B and D produced similar response as that of program C. Results for sealed fiber (red line) is replotted in inset for clarity. Scan rate for each CV was 25 mV/s.

The separation between the cathodic and anodic peaks was found to be 70 mV, which is larger than the expected 59 mV for this faradaic reversible one-electron reaction.[62] Velmurugan et al. reported similar findings in their study of electrochemistry through glass using platinum nanoelectrodes.[64] They found the peak separation for the $Ru(NH_3)_6^{3+}/Ru(NH_3)_6^{2+}$ redox couple to be 95 mV, and concluded that the 35mV increase in peak separation over the expected value is related to the resistance of the thin glass layer that hinders transport of the redox probe to the electrode surface. The cathodic and anodic peaks for ferrocene methanol were centered at 0.280 V vs. Ag/AgCl, which is 80 mV more positive than that which has been previously reported using other electrode systems.[65] This also may be related to the glass layer at the electrode surface since it was previously reported by Lowinsohn et al.[66] that the position of the $FcMeOH/FcMeOH^+$ redox

couple can shift by up to 140 mV more positive than expected when the electrode surface is modified in a way that affects hydrophobicity.

## Post-Pulling Treatment Methods to Expose Insulated Carbon Fibers

Since pulling programs B, C, and D resulted in fibers that were completely insulated by glass, post-pulling treatments were necessary to remove glass insulation and expose the conductive fiber in order to produce electrodes. Post-pulling treatments were also applied to electrodes prepared using pulling program A in an attempt to improve electrochemical response. Two post-pulling treatment procedures, flame etching and mechanical polishing, were carried out on separate sealed fibers in order to test their efficacy for producing small electrodes.

### Flame Etching of Carbon Fiber

Flame etching was completed by directing a butane flame onto the sealed fiber for ~5 s. Sealed fibers produced from pulling programs B, C, and D were sufficiently exposed after flame etching to produce carbon UMEs (Figure 7) with limiting currents for FcMeOH oxidation ranging from 100-450 pA. Flame etching of electrodes produced using program A parameters also resulted in sigmoidal-shaped CV response with ~200 pA limiting current for the FcMeOH/$FcMeOH^+$ redox couple, which further supports the idea that electrodes prepared directly by program A may have been covered by a thin layer of glass immediately after pulling.

In the case of electrodes prepared from program A, flame etching was capable of removing the thin glass layer from the electrode, resulting in expected sigmoidal-shaped UME behavior (Figure 7A) instead of the previously observed peak-shaped response (Figure 6). Limiting currents observed for oxidation of FcMeOH using electrodes prepared from various pulling parameters and subsequent flame etching correspond to electrode radius ranging from 230 nm to 390 nm. The

smallest electrodes resulted from program C, which produced a more pointed tip with little glass insulator around the carbon fiber.

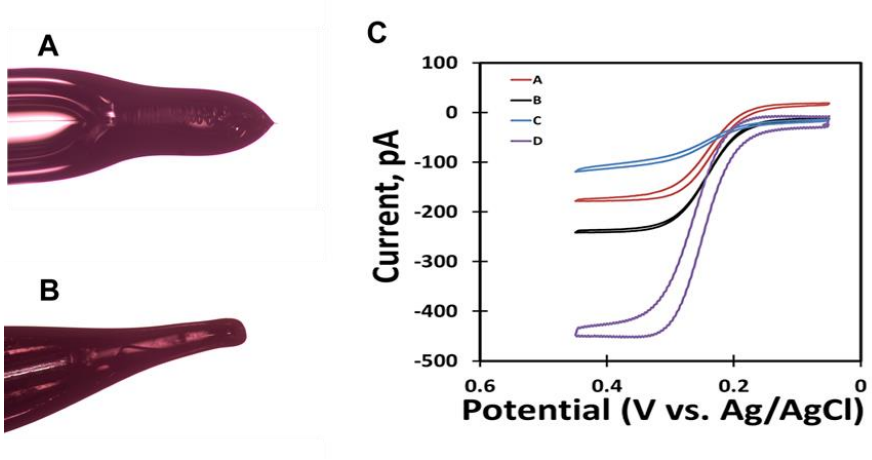


**Figure 7:** Appearance and electrochemical response of flame-etched electrodes. Images depict an electrode produced using program C before (A) and after (B) flame etching. C) Representative CVs of flame-etched electrodes in 0.5mM FcMeOH in 0.1M KCl. Scan rate = 25 mV/s.

Manual Mechanical Polishing to Expose Carbon Fiber

Manual mechanical polishing on 800-grit abrasive paper was employed as an alternative method to expose sealed carbon fibers. Polishing was carefully done in a circular manner. Like flame etching, polishing also led to exposure of sealed carbon fibers to produce UMEs (Figure 8).

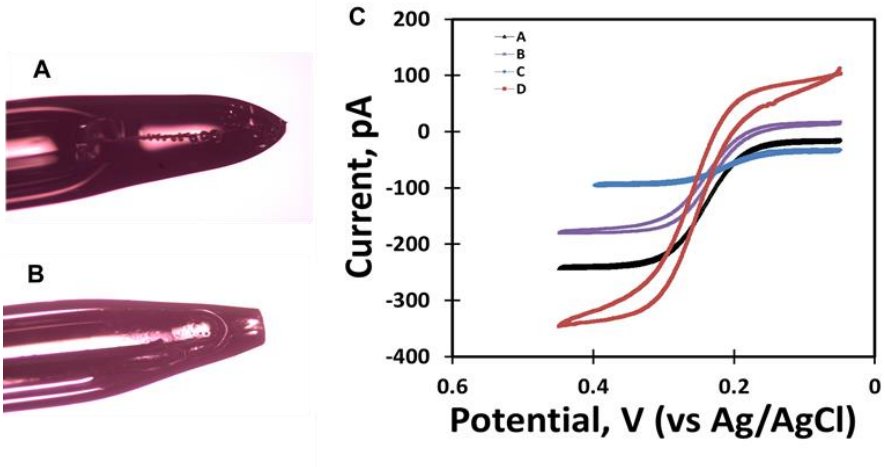


**Figure 8:** Appearance and electrochemical response for electrodes produced by manual polishing. Images depict an electrode prepared using program before (A) and after (B) manual polishing. C) Representative CVs of manually polished electrodes in 0.5 mM FcMeOH and 0.1M KCl. Scan rate = 25 mV/s.

Limiting currents for the FcMeOH/FcMeOH$^+$ redox couple using electrodes produced by polishing were generally smaller than those obtained using electrodes prepared from the same set of pulling conditions coupled with flame etching. Limiting currents for polished carbon fiber UMEs ranged from 60-350 pA, corresponding to sizes of 200 nm to 360 nm. As with flame-etching, pulling program C produced the smallest electrode (Figure 9 and Table3).

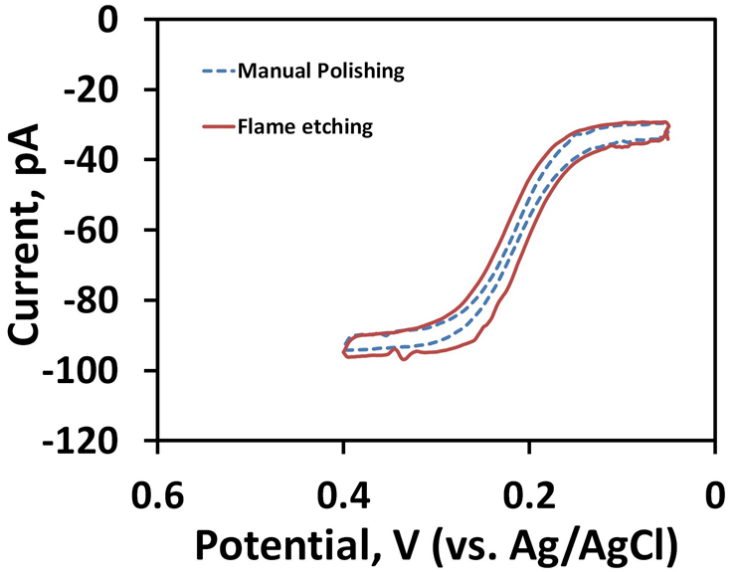


**Figure 9:** Representative CV responses of 0.50 mM ferrocene methanol in 0.10 M KCl using ultramicroelectrodes with <250 nm radii produced by both manual polishing and flame etching. Small manually polished (blue line) and flame etched (red line) electrodes were both prepared using program C. Scan rate is 25 mV/s.

**Table 3**: Minimum sizes (radii in nm) of electrodes prepared from different pulling programs and post-treatment techniques

| Program | Manual Polishing | Flame Etching |
|---|---|---|
| A | 270 | 260 |
| B | 260 | 280 |
| C | 200 | 230 |
| D | 390 | 360 |

Effects of Post-Pulling Treatment Techniques on Electrode Reproducibility

Another vital challenge in nanoelectrode fabrication is reproducibility. Size variability of electrodes made by manual polishing and flame etching was evaluated by comparing

electrochemical responses of identically prepared and post-pulling-treated electrodes. In total, 20 capillaries with fibers sealed using pulling program C were prepared, and 10 each were treated using manual polishing and flame etching to produce carbon UMEs. Electrode sizes were determined based on CV response towards FcMeOH oxidation (Table 4).

**Table 4:** Variations in carbon fiber UME size for electrodes prepared using different post-pulling treatment strategies

| Treatment | Functional Electrodes (out of 10) | Average Radius (nm) (± Standard Deviation) |
|---|---|---|
| Flame etching | 4 | 250 (± 15) |
| Manual polishing | 7 | 214 (± 9) |

The average size of manually polished electrodes was slightly smaller but significantly different (at the 95% confidence limit) than that of flame-etched electrodes. Though both methods exhibited variation in electrode size of <7% based on relative standard deviation, the success rate of producing functional electrodes through manual mechanical polishing (70%) was greater than that using flame etching (40%). Overall, manual polishing produced smaller electrodes and proved to be more controllable than flame etching since measurements could be taken periodically during the process until a desired (sigmoidal-shaped) response was obtained. With flame etching, the short time needed for fiber exposure and lack of control over flame properties that affect melting of the glass and etching of the fiber made it more difficult to control electrode fabrication.

## Electrochemical Responses from CVD Electrodes

Since sealing of carbon fibers in glass capillaries and exposure of electrode surface through post-treatment strategies led to electrodes with sizes of 200 nm or greater, chemical vapor deposition (CVD) was explored as an alternative for making smaller electrodes. Quartz capillaries (I.D. 0.30 mm) were processed using the laser-based pipette puller to produce capillary pipettes

with tapered ends. For pipette preparation, typical pulling parameters were Heat: 850, Filament: 4, Velocity: 36, Delay: 140, and Pull: 50. CVD was carried out inside the quartz capillary at the tapered end using a butane microtorch to heat a propane-butane mixture,[44] which resulted in carbon UMEs.

Types of Responses Associated with Electrodes Prepared by the CVD Method

Two general types of electrochemical responses were obtained from carbon-filled pipettes prepared by CVD. Sigmoidal responses towards the FcMeOH/FcMeOH$^+$ redox couple, which were expected and are indicative of disk-shaped carbon UMEs, were most often obtained (Figure 10). The second type of response had an unusual combination of small faradaic current with a peak-shaped response when CVs were conducted at a scan rate of 25 mV/s (Figure 11A). However, in contrast with carbon fiber electrodes prepared by laser-assisted pulling using program A which exhibited a similar behavior (Figure 6), the peaks in this case were centered at 0.200 V vs. Ag/AgCl as expected, and the peak separation of 2 mV was less than the theoretical value (59 mV). Interestingly, a sigmoidal response was obtained when CVs were conducted at a scan rate of 10 mV/s for the same electrode in FcMeOH (Figure 11B).

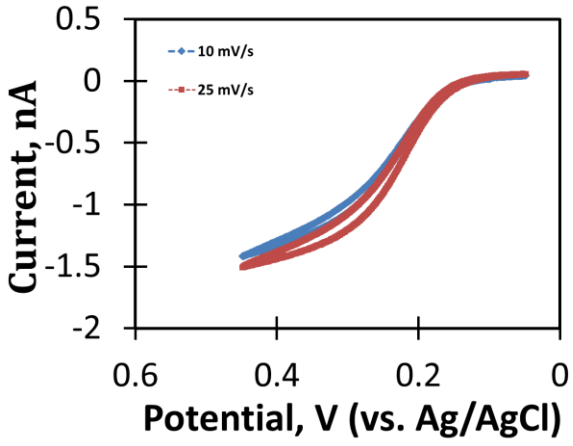


**Figure 10:** CV responses of 0.5 mM FcMeOH in 0.1 M KCl solution obtained using a CVD UME at different potential sweep rates. Scan rate = 10 mV/s (blue line) and 25 mV/s (red line).

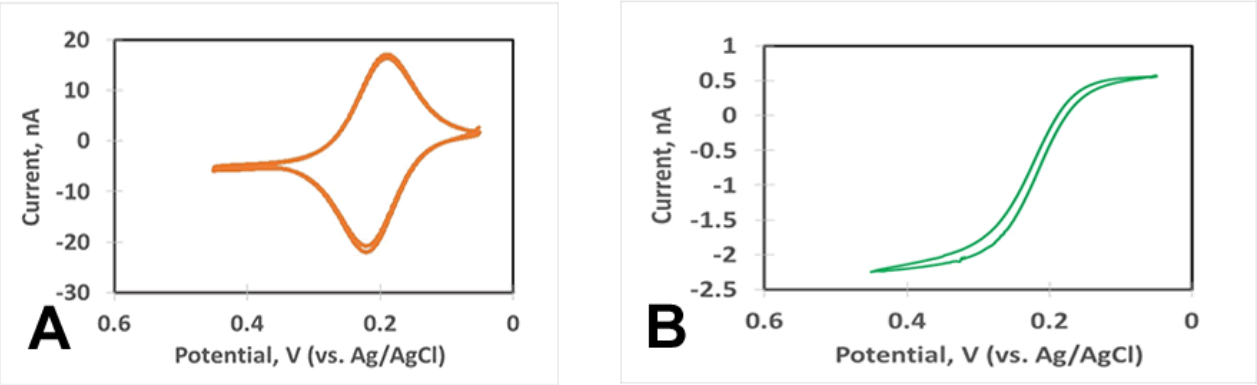


**Figure 11:** Scan-rate dependent CV responses of CVD carbon electrodes prepared by under deposition of carbon in the pipette tip. A) Peak-shaped form of response using a scan rate of 25 mV/s. B) Sigmoidal-shaped form of response using a scan rate of 10 mV/s.

The scan rate dependence of the shape of the CV signal is consistent with CV behavior that has been previously described for carbon nanosampler electrodes prepared by CVD. Yu et al.[49] showed that such nanosampler electrodes could be prepared using CVD by limiting the deposition time so that the thin layer of carbon deposited on the inside of the pipette at the tapered opening forms a carbon nanoring with a nanometer-sized cavity in the center rather than a disk. The cavity enables solution to be drawn in to the pipette tip creating contact with the electrode.

The electrochemical behavior of nanosampler electrodes at relatively high CV scan rates essentially mimics that of an electrode with a thin layer of redox species immobilized on the surface, which similarly exhibit peak-shaped response and peak separation values of around 0 mV.[49] For nanosampler electrodes, the forward (anodic) peak is higher in magnitude than that of the reverse (cathodic) peak because of the additional steady-state anodic component of the sigmoidal curve. This asymmetrical nature of peaks results from the inclusion of steady-state diffusion current to the pipette orifice (Figure 11B). Again, CV shape here is strongly dependent on the scan rate. Curve B in Figure 11 generated at a scan rate of 10 mV/s is totally sigmoidal, and it can be difficult to distinguish this response from similar voltammograms obtained from disk-shaped

nanoelectrodes. The sigmoidal behavior at slow scan rates is due the contribution of quasi-spherical diffusion to the carbon nanoring from the redox species in the bulk solution.[49]

Responses from Functional CVD Electrodes Used in Size Estimation

Every pull produced a pipette pair (one each from both left and right puller arms of the laser-assisted puller), and pipettes in each pair were processed using CVD in the same way to produce electrodes. Electrodes obtained from left puller arm (blue curve) gave a smaller electrochemical response towards the $FcMeOH/FcMeOH^+$ redox couple than those from the right puller arm (red curve) (Figure 12).

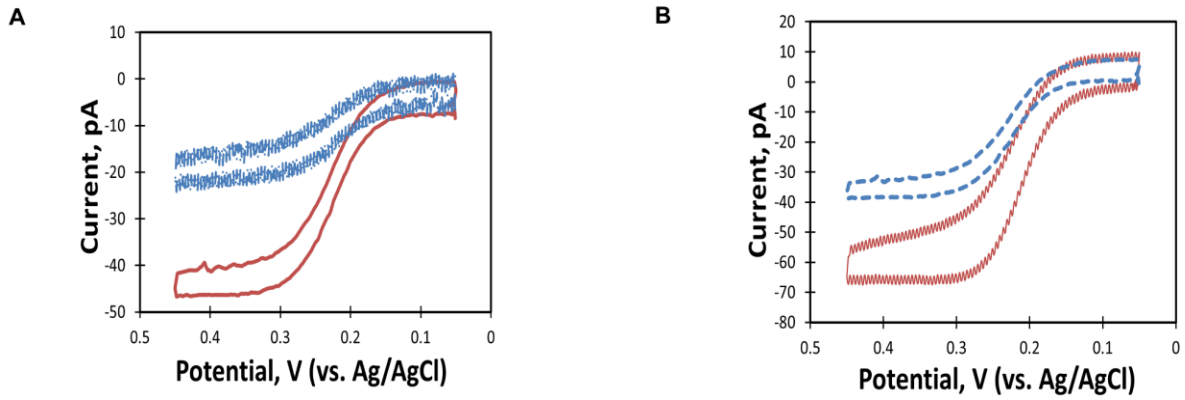


**Figure 12:** Representative CVs of CVD disk-shaped carbon ultramicroelectrodes comparing sizes of twin electrodes. Blue curves represent voltammograms from the left pulling arm. Red curve voltammograms are those obtained from the right pulling arm. Scan rate is at 25 mV/s.

Electrodes made from the left part of the pulling compartment gave steady-state diffusion current of 20 and 35 pA corresponding to radii of 130 and 230 nm compared to their right arm counterparts with 35and 65 pA representing electrode radii of 290 and 430 nm. This significant difference in electrode size may be due to uneven melting of glass during pulling or unequal deposition of carbon and melting of quartz pipette by butane flame, which occur during the CVD process. Mirkin's group[55] explained that localized heating at the small tapered end of pulled capillary tubes during CVD of carbon carried out in a tube furnace at a temperature of 900 ˚C helps

reduce electrode size. However, this process may also lead to size variations. The butane flame used in this work possesses a higher temperature (1430 ˚C) than the tube furnace, so melting of quartz during CVD is reasonable. Further work was done by adjusting deposition time which led to the production of a nanoelectrode with radius 50 nm (Figure 13).

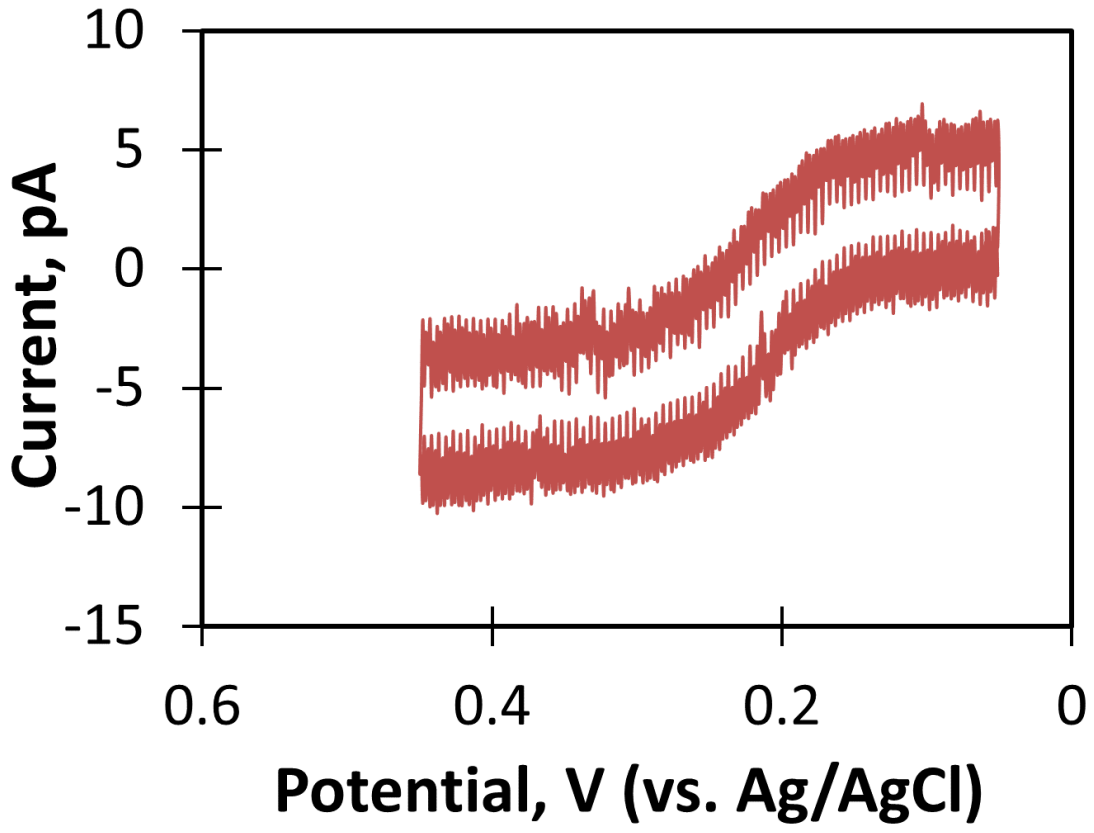


**Figure 13:** Representative CV from the smallest CVD electrode of 0.50 mM ferrocene methanol in 0.10 M KCl

# CHAPTER 4

# CONCLUSIONS

Nanomaterials can exhibit enhanced catalytic properties for various chemical and electrochemical reactions compared to bulk materials due to their relatively large surface area-to-volume ratios. The relationships between physical and catalytic properties of nanoparticles have been determined through research using collections of nanoparticles deposited on solid supports. But, these ensemble measurements may create important barriers in nanoparticle characterization. In contrast, catalytic properties of nanoparticles determined at the single nanoparticle level should enable easier and more reliable evaluations and comparisons of nanoparticle structure-function relationships.

Recent advances in electrochemical techniques have enabled evaluation of the electrocatalytic properties of individual nanoparticles. These electrocatalytic measurements on single nanoparticles have been performed through evaluation of transient currents that develop as single nanoparticles impact UMEs and through single nanoparticle voltammetry accomplished by immobilizing single nanoparticles on nanoelectrodes. Carbon is desirable as a platform for immobilizing single metal nanoparticles since it is not catalytically active towards many electrochemical reactions promoted by metal nanoparticles and thus does not interfere in the electrochemical response obtained from metal particles during studies of electrocatalysis.

In these studies, sealing of carbon fibers in borosilicate glass capillary tubes and chemical vapor deposition of carbon in quartz tapered capillary tubes were investigated and compared as methods for preparing carbon ultramicro- and nanoelectrodes. Both techniques required use of a laser-based pipette puller. Four pulling programs were found to provide adequate sealing of the carbon fiber in the glass capillary tube. Although these four pulling programs effectively sealed

carbon fibers in glass capillaries to produce durable and stable electrodes, only those fabricated from program A produced electrodes that gave electrochemical response towards FcMeOH redox probe immediately after pulling. However, these electrodes exhibited peak-shaped response instead of the expected sigmoidal response, which indicated that the fiber may have been coated with a thin layer of glass.[53]

Post-pulling treatments were applied to expose carbon fibers that were completely sealed or seemingly obscured by a thin glass layer. Flame etching and manual mechanical polishing were employed to further expose and etch carbon fibers in order to produce electrodes with radii of 200-390 nm. Though both post treatment techniques yielded functional electrodes, a higher success rate in electrode fabrication was exhibited by manual mechanical polishing.

Chemical vapor deposition (CVD) of carbon in quartz Ultramicro- and nanopipettes was also investigated as a method for preparing UMEs. Carbon electrodes produced by CVD could be fabricated in shorter time and required no post-treatment. The electrochemical behavior of CVD carbon UMEs depended on carbon deposition time. The smallest of electrode made from this fabrication technique was of radius 50 nm which is about four times smaller than the smallest electrode prepared from laser assisted pulling of carbon fiber. Though the applied pulling program consistently produced electrodes with desired responses, the CVD method proved not to be as reproducible from this work, which is evident in the exhibited large variations from CVs of these twin electrode pairs. In contrast, Actis et al.[44] investigated the reproducibility of nanoelectrodes prepared from CVD by the same strategy reported here. CVD electrodes prepared from pipettes produced by the same pulling parameters were reported to show relatively narrow size distribution with an average radii of 30 (± 4) nm. CVs from fabricated twin electrodes exhibited good agreement with little variations for all sets of electrodes.

Though both electrode fabrication methods were successful, CVD of carbon proved to be a simpler and easier approach than the sealing of carbon fiber in a glass capillary through laser-assisted pulling. The electrodes prepared in these studies may be employed in nanoparticle impact studies, but the sizes are likely too large for immobilization of single nanoparticles. To produce smaller electrode sizes, beveling (a more automated and controllable mechanical polishing post-pulling treatment technique) will be applied to carbon fiber electrodes and the usage of furnace (with controllable temperature) for the deposition of carbon will be carried out for the CVD method.

REFERENCES


1. Niu, Z.; Li, Y. Removal and Utilization of Capping Agents in Nanocatalysis. *Chem. Mater.* **2014,** *26,* 72-83.

2. Yu, Y.; Gao, Y.; Hu, K.; Blanchard, P.Y.; Noel, J.M; Nareshkumar, T.; Phani, K. L.; Friedman, G.; Gogotsi, Y.; Mirkin, M. V. Electrochemistry and Electrocatalysis at Single Gold Nanoparticles Attached to Carbon Nanoelectrodes, *Chem. Electro. Chem*. **2015,** *2,* 58-63.

3. McKelvey, K.; German, S. R.; Zhang, Y.; White, H. S.; Edwards, M. A. Nanopipettes as a Tool for Single Nanoparticle Electrochemistry, *Curr. Opin. Electrochem.* **2017,** *6,* 4-9.

4. Dayton, M. A.; Brown, J. C.; Stutts, K. J.; Wightman, R. M. Faradaic Electrochemistry at Microvoltammetric Electrodes. *Anal. Chem*. **1980,** *52,* 946−950.

5. Anderson, T. J.; Zhang, B. Single-Nanoparticle Electrochemistry Through Immobilization and Collision. *Acc. Chem*. *Res.* **2016,** *49,* 2625-2631.

6. Xiao, X.; Pan, S.; Jang, J.S.; Fan, F.-R.F.; Bard, A.J. Single Nanoparticle Electrocatalysis: Effect of Monolayers on Particle and Electrode on Electron Transfer. J. Phys. Chem. C, **2009,** *113,* 14978-14982.

7. Xu, W.; Kong, J.S.; Chen, P. Probing the Catalytic Activity and Heterogeneity of Au-Nanoparticles at the Single-Molecule Level. *Phys. Chem. Chem. Phys.* **2009,** *11,* 2767-2778.

8. Xiao, X.; Bard, A.J. Observing Single Nanoparticle Collisions at an Ultramicroelectrode by Electrocatalytic Amplification. *J. Am. Chem. Soc*. **2007,** 129, 9610-9612.

9. Zhou, H.; Fan, F.-R.F.; Bard, A.J.; Observation of Discrete Au Nanoparticle Collisions by Electrocatalytic Amplification using Pt Ultramicroelectrode Surface Modification. *J. Phys. Chem*. **2010,** *1,* 2671-2674.

10. Kwon, S.J.; Zhou, H.; Fan, F.-R.F.; Vorobyev, V.; Zhang, B., Bard, A.J.; Stochastic Electrochemistry with Electrocatalytic Nanoparticles at Inert Ultramicroelectrodes – Theory and Experiments. *Phys. Chem. Chem. Phys*. **2011,** *13,* 5934-5402.

11. Rees, N.V.; Zhou, Y.-G.; Compton, R.G. Making Contact: Charge Transfer During Particle-Electrode Collisions. *RSC Adv*. **2012,** *2,* 379-384.

12. Cheng, W.; Compton, R.G.; Electrochemical Detection of Nanoparticles by 'Nano-Impact' Methods. *Trends Anal. Chem.* **2014,** *58,* 79-89.

13. Kleijn, S.E.F.; Serrano-Bou, B.; Yanson, A.I.; Koper, M.T.M. Influence of Hydrazine-Induced Aggregation the Electrochemical Detection of Platinum Nanoparticles. *Langmuir,* **2013,** *29,* 2054-2064.

14. Dasari, R.; Robinson, D.A.; Stevenson, K.J. Ultrasensitive Electroanalytical Tool for Detecting, Sizing, and Evaluating the Catalytic Activity of Platinum Nanoparticles. *J. Am. Chem. Soc.* **2013,** *135,* 570-573.

15. Chen, C.-H.; Ravenhill, E.R.; Momotenko, D.; Kim, Y.-R.; Lai, S.C.S.; Unwin, P.R.; Impact of Surface Chemistry on Nanoparticle – Electrode Interactions in the Electrochemical Detection of Nanoparticle Collisions. *Langmuir* **2015,** *31,* 11932-11942.

16. Robinson, D.A.; Kondajji, A.M.; Casteñeda, A.D.; Dasari, R.; Crooks, R.M.; Stevenson, K.J. Addressing Colloidal Stability for Unambiguous Electroanalysis of Single Nanoparticle Impacts. *J. Phys. Chem.* **2016,** *7,* 2512-2517.

17. Zoski, C. G.; Liu, B.; Bard, A. Scanning Electrochemical Microscopy: Theory and Characterization of Electrodes of Finite Conical Geometry. *Anal. Chem.* **2004,** *76,* 3646-3654.

18. Wehmeyer, K. R.; Deakin, M. R.; Wightman, R. M. Eletroanalytical Properties of Band Electrodes of Sub Micrometer Width. *Anal. Chem*. **1985,** *57,* 1913-1916.

19. Lin, C.; Katelhon, E.; Sepunaru, L.; Compton, R. G. Understanding Single Enzyme Activity via the Nano Impact Technique. *Chem. Sci.* **2017,** *8,* 6423-6432.

20. Oja, S.M.; Fan, Y.; Armstrong, C.M.; Defnet, P.; Zhang, B. Nanoscale Electrochemistry Revisited. *Anal. Chem.* **2016,** *88,* 414-430.

21. Sun, P.; Li, F.; Yang, C.; Sun, T.; Kady, I.; Hunt, B.; Zhuang, J. Formation of a Single Gold Nanoparticle on a Nanometer-Sized Electrode and its Electrochemical Behaviors. *J. Phys. Chem. C* **2013,** *117,* 6120-6125.

22. Li, Y.; Cox, J.T.; Zhang, B. Electrochemical Responses and Electrocatalysis at Single Au Nanoparticles. *J. Am. Chem. Soc.* **2010,** *132,* 3047-3054.

23. Dayton, M. A.; Ewing, A. G.; Wightman, R. M. Response of Microvoltammetric electrodes to Homogeneous Catalytic and Slow Heterogeneous Charge-Transfer Reactions**.** *Anal. Chem*. **1980,** *52,* 2392-2396.

24. Dayton, M. A.; Brown, J. C.; Stutts, K. J.; Wightman, R. M. Faradaic Electrochemistry at Microvoltammetric Electrodes. *Anal. Chem*. **1980,** *52,* 946-950.

25. Bond, A. M.; Fleischmann, M.; Robinson, J. Electrochemistry in Organic Solvents without Supporting Electrolyte using Platinum Microelectrodes. *J. Electroanal. Chem.* **1984,** *168,* 299-312.

26. Kittlesen, G. P.; White, H. S.; Wrighton, M. S. Chemical Derivatization of Microelectrode Arrays by Oxidation of Pyrrole and N-Methylpyrrole: Fabrication of Molecule-Based Electronic Devices *J. Am. Chem. Soc***. 1984,** *106,* 7389-7396.

27. Oja, S. M.; Wood, M.; Zhang, B. Nanoscale Electrochemistry, *Anal. Chem.* **2013,** *85*, 473-486.

28. Selzer, Y.; Mandler, D. Scanning Electrochemical Microscopy. Theory of the Feedback Mode for Hemispherical Ultramicroelectrodes: Steady-State and Transient Behavior *Anal. Chem*. **2000,** *72*, 2383-2390.

29. Macpherson, J. V.; Jones, C. E.; Unwin, P. R. *J. Phys. Chem. B* **1998,** *102*, 9891-9897.

30. Zhang, B.; Zhang, Y.; White, H. S. The Nanopore Electrode. *Anal. Chem*. **2004,** *76*, 6229-6238.

31. Penner, R. M.; Heben, M. J.; Longin, T. L.; Lewis, N. S. Fabrication and Use of Nanometer-Sized Electrodes in Electrochemistry. *Science* **1990,** *250*, 1118-1121.

32. Mirkin, M. V.; Fan, F.-R. F.; Bard, A. J. Evaluation of the Tip Shapes of Nanometer size Microelectrodes. *J. Electroanal. Chem*. **1992,** *328*, 47-62.

33. Sun, P.; Zhang, Z.; Guo, J.; Shao, Y. Fabrication of Nanometer-Sized Electrodes and Tips for Scanning Electrochemical Microscopy. *Anal. Chem*. **2001,** *73*, 5346-5351.

34. Watkins, J. J.; Chen, J.; White, H. S.; Abruňa, H. D.; Maisonhaute, E.; Amatore, C. Fabrication of Nanometer-Sized Electrodes and Tips for Scanning Electrochemical Microscopy. *Chem Anal.* **2003,** *75*, 3962-3971.

35. Shao, Y.; Mirkin, M. V.; Fish, G.; Kokotov, S.; Palanker, D.; Lewis, A. Nanometer-Sized Electrochemical Sensors. *Anal. Chem*. **1997,** *69*, 1627-1634.

36. Noel, J.; Velmurugan, J.; Gokmese, E.; Mirkin, M. V. *J. Solid State Electrochem.* **2013,** *17*, 385-389.

37. Katemann, B. B.; Schuhmann, W. Fabrication and Characterization of Needle-Type Pt-Disk Nanoelectrodes. *Electroanalysis* **2002,** *14*, 22-28.

38. Ying, Y. L.; Ding, Z.; Zhan, D.; Long, Y. T. Advanced Electroanalytical Chemistry at Nanoelectrodes. *Chem. Sci.* **2017,** *8*, 3338-3348.

39. Schroeder, T. J.; Jankowski, J. A.; Senyshyn, J.; Holz, R. W.; Wightman, R.M. Zones of Exocytotic Release on Bovine Adrenal Medullary Cells in Culture. *J. Biol. Chem.* **1994,** *269*, 17215-17220.

40. Huang, W. H.; Pang, D. W.; Tong, H.; Wang, Z. L.; Cheng, J. K.; A Method for the Fabrication of Low-Noise Carbon Fiber Nanoelectrodes. Anal. Chem. **2001,** *73*, 1048-1052.

41. Zhang, X. J.; Zhang, W. M.; Zhou, X. Y.; Ogorevc, B. Fabrication, Characterization, and Potential Application of Carbon-Fiber Cone Nanometer-Size Electrodes. *Anal. Chem*. **1996**, *68*, 3338-3343.

42. Li, Y. Z.; Zhoua, W.; Wua, Z. X.; Zhanga, R. Y.; Xua, T. Fabrication of Size-Controllable Ultrasmall-Disk Electrode: Monitoring single Vesicle Release Kinetics at Tiny Structures with High Spatio-Temporal Resolution. *Biosens. Bioelectron.* **2009,** *24,* 1358-1364.

43. Agyekum, I.; Nimley, C.; Yang, C.; Sun, P. Combination of Scanning Electron Microscopy in the Characterization of a Nanometer-Sized Electrode and Current Fluctuation Observed at a Nanometer-Sized Electrode. *J. Phys. Chem.* **2010,** *114,* 14970-14974.

44. Actis, P.; Tokar, S.; Clausmeyer, J.; Babakinejad, B.; Mikhaleva, S.; Cornut, R.; Takahashi, Y.; Córdoba, A. L.; Novak, P.; Shevchuck, A. I.; Dougan, J. A.; Kazarian, S. G.; Gorelkin, P. V.; Erofeev, A. S.; Yaminsky, I. V.; Unwin, P. R.; Schuhmann, W.; Klenerman, D.; Rusakov, D. A.; Sviderskaya, E. V.; Korchev, Y. E. Electrochemical Nanoprobes for Single-Cell Analysis**.** *ACS Nano*, **2014,** *8,* 875-884.

45. Kim, Y. T.; Scarnulis, D. M.; Ewing, A. G. Carbon-Ring Electrodes with One-Micrometer Tip Diameter. *Anal. Chem.* **1986,** *58,* 1782-1786.

46. Takahashi, Y.; Shevchuk, A. I.; Novak, P.; Zhang, Y.; Ebejer, N.; Macpherson, J. V.; Unwin, P. R.; Pollard, A. J.; Roy, D.; Clifford, C. A.; Shiku, H.; Matsue, T.; Klenerman, D.; Korchev, Y. E. *Angew. Chem., Int. Ed*. **2011,** *50,* 9638-9642.

47. Rees, H. R.; Anderson, S. E.; Privman, E.; Bau H. H.; Venton, B. J. Carbon Nanopipette Electrodes for Dopamine Detection in Drosophila. *Anal. Chem*. **2015,** *87,* 3849-385.

48. Singhal, R.; Bhattacharyya, S.; Orynbayeva, Z.; Vitol, E.; Friedman, G.; Gogotsi, Y. Small Diameter Carbon Nanopipettes. *Nanotechnology* **2010**, *21,* 015304.

49. Yu, Y.; Noel, J. M.; Mirkin, M.V. Carbon Pipette-Based Electrochemical Nanosampler. *Anal. Chem.* **2014,** *86,* 3365-3372.

50. Morton, K. C.; Morris, C. A.; Derylo, M. A.; Thakar, R.; Baker, L. A. Carbon Electrode Fabrication from Pyrolyzed Parylene C. *Anal. Chem.* **2011,** *83,* 5447-5452.

51. Demaille, C.; Brust, M.; Tsionsky, M.; Bard, A. Fabrication and Characterization of Self-Assembled Spherical Gold Ultramicroelectrodes. *Anal. Chem.* **1997,** *69,* 2323-2328.

52. Jena, B. K.; Percival, S. J.; Zhang, B. Au Disk Nanoelectrode by Electrochemical Deposition in a Nanopore. *Anal. Chem.* **2010,** *82,* 6737-6743.

53. Velmurugan, J.; Mirkin, M. V. Fabrication of Nanoelectrodes and Metal Clusters by Electrodeposition. *Chem. Phys. Chem.* **2010,** *11,* 3011-3017.

54. Hao, R.; Zhang, B. Nanopipette-Based Electroplated Nanoelectrodes. *Anal. Chem.* **2015,** *88,* 614-620.

55. Chen, R.; Hu, K.; Yu, Y. Mirkin V. M.; Ameyiya, S. Focused-Ion-Beam-Milled Carbon Nanoelectrodes for Scanning Electrochemical Microscopy. *J. Electrochem Soc.* **2016,** *163,* H3032-H3037.

56. Li, Y.; Bergman, D.; Zhang, B. Preparation and Electrochemical Response of 1−3 nm Pt Disk Electrodes**.** *Anal. Chem.* **2009,** *81,* 5496–5502.

57. Anderson, S. E.; Bau, H. H. Carbon Nanoelectrodes for Single-Cell. *Nanotechnology* **2015,** *26,* 185-195.

58. Fei, J.; Wua, K.; Wang, F.; Hu, S. Glucose Nanosensors Based on Redox Polymer/Glucose Oxidase Modified Carbon Fiber Nanoelectrodes. *Talanta* **2005,** *65,* 918-924.

59. Mirkin, M. V. Nanoelectrodes and Liquid/Liquid Nanointerfaces. In *Nanoelectrochemistry*; Mirkin, M. V., Amemiya, S., Eds.; CRC Press, Boca Raton, FL, **2015;** pp. 539-572.

60. Sutter Instrument Co. P-2000 Micropipette Puller, **2012,** Rev 2.4, pp 16-17.

61. Dayton, M. A.; Brown, J. C.; Stutts, K. J.; Wightman, R. M. Faradaic Electrochemistry at Microvoltammetric Electrodes. *Anal. Chem*. **1980,** *52,* 946-950.

62. Skoog, D. A.; Holler, F. J.; Crouch, S. R. Principles of Instrumental Analysis, 6th ed.; Cengage Learning: Stamford, **2007;** pp 726-729.

63. Morris, C. A.; Friedman, A. K.; Baker, L. A. Applications of Nanopipettes in the Analytical Sciences. *Analyst* **2010,** *135,* 2190-2202.

64. Velmurugan, J.; Zhan, D.; Mirkin, M. V. Electrochemistry Through Glass. *Nat. Chem.* **2010,** *2,* 498- 502.

65. Norouzi, P.; Faridbod, F.; Larijani, B.; Ganjali, M. R. Glucose Biosensor Based on MWCNTs-Gold Nanoparticles in a Nafion Film on the Glassy Carbon Electrode Using Flow Injection FFT Continuous Cyclic Voltammetry. *Int. J. Electrochem. Sci.* **2010,** *5,* 1213-1224.

66. Lowinsohn, D.; Gan, P.; Tschulik, K.; Foord, J. S.; Compton, R. G. Nanocarbon Paste Electrodes. *Electroanalysis* **2013,** *25,* 2435-2444.

# VITA

## THEOPHILUS NEEQUAYE

Education:

MS Chemistry, East Tennessee State University, Johnson City, TN, 2018
B.Sc. Chemistry, Kwame Nkrumah University of Science and Technology, Kumasi, Ghana, 2013

Professional Experience:

Graduate Teaching Assistant, East Tennessee State University, Johnson City, TN, 2016-2018
Production Supervisor, M&G Pharmaceuticals Limited, Accra, Ghana, 2015-2016
Integrated Science and Mathematics Teacher, Achiaman MA School, Amasaman, Ghana, 2013-2014

Research Experience:

Graduate Research Student, East Tennessee State University, Johnson City, TN, 2016-2018 (Mentor: Dr. Gregory W. Bishop)

- Prepared ultramicro- and nanoelectrodes from carbon fiber and chemical vapor deposition of carbon
- Synthesized gold nanoparticles
- Investigated strategies for modifying carbon electrodes with nanoparticles

Undergraduate Research Student, Kwame Nkrumah University of Science and Technology, Kumasi, Ghana, 2012-2013 (Supervisor: Prof. Anthony Adimado)

- Evaluated airborne lead in electric arc welding environments

Presentations:

T. Neequaye, G. Affadu-Danful, and G. W. Bishop, "Preparation and Characterization of Carbon Ultramicroelectrodes for Electrocatalytic Studies of Single Gold Nanoparticles," 69th South Eastern Regional Meeting of the American Chemical Society, 11/09/2017, Charlotte, NC, Poster Presentation 552

T. Neequaye, "Comparing Bottom-Up and Top-Down Approaches in the Fabrication and Characterization of Carbon Ultramicroelectrodes," East Tennessee State University Department of Chemistry Seminar, 03/23/2018, Johnson City, TN, Oral Presentation

T. Neequaye, G. Affadu-Danful, and G. W. Bishop "Investigations of Pre- and Post-Treatment Protocols in the Fabrication of Carbon Fiber Ultramicro- and Nanoelectrodes," Appalachian Student Research Forum, 04/04/2018, Johnson City, TN, Oral Presentation